

ANOMALOUS ELECTRICAL TRANSPORT PROPERTIES OF C_{54} -TiSi₂ FILMS MEASURED BY THE VAN DER PAUW METHOD

Jeng-Rern YANG

Department of Electrical Engineering, National Tsing Hua University, Hsinchu, Taiwan, ROC

Juh-Tzeng LUE

Department of Physics, National Tsing Hua University, Hsinchu, Taiwan, ROC

and

In-Chin WU

Materials Science Center, National Tsing Hua University, Hsinchu, Taiwan, ROC

Received 23 March 1987; revised manuscript received 5 February 1988; accepted for publication 13 May 1988

Communicated by J.I. Budnick

We have measured the temperature dependence of the electrical resistivity and Hall constant of single phase C_{54} -TiSi₂ films on (111) silicon wafers prepared by isothermal annealing at 800°C in vacuum. The temperature dependence of the electrical resistivity follows the Bloch-Grüneisen equation but has a striking dip for the short time annealed samples. We find that the magnitude of the Hall constant $|R_H|$ increases as the temperature decreases from above the Debye temperature and reaches a maximum value and then decreases until reversing sign at lower temperatures. A two-band model and size effect can qualitatively explain this anomalous result.

Recently, metal base-transistors (MBT) have been successfully fabricated by Tung et al. [1] which are considered to be the essential parts for constructing three dimensional integrated circuits (3DIC). To obtain a high-common base current gain α_0 , the thickness of the silicide should be less than the mean free path in bulk silicide causing unnoticed surface scattering and size effect. Epitaxial growth of TiSi₂ on local spots [2] has been shown to have the lowest resistivity [3] in transition-metal silicides revealing itself as a potential material in the fabrication of 3D integrated circuits. Till now the treatment of carrier transport mechanism has been largely heuristic and superficial. Although Malhotra et al. have measured the temperature dependent resistivity of TiSi₂ [4] and observed the galvano-magnetic and Hall effects on Corbino disk samples at a specified annealing condition, they have hastily discarded the isotropic two-band model just for a single data taking at room temperature.

In a previous work [5], we have reported the refractive index of titanium silicides within visible light. In order to obtain more insight into the carrier transport properties we have measured the temperature dependence of electrical resistivity and Hall constants of TiSi₂ at different annealing times. We have found the anomalous resistivity and sign reversal of the Hall constant.

Titanium films with a thickness of 200 Å were electron-gun deposited on (111), 1–10 Ω cm silicon substrates under a pressure of 1×10^{-6} Torr at a deposition rate of 2 Å/min. The samples were isothermally annealed at 800°C for 6, 30 and 240 min, respectively in an oil-free high vacuum furnace. The TEM electron diffraction pattern and SEM (scanning electron microscope) cross-sectional view indicate that the Ti silicides are face-centered orthorhombic C_{54} with $a_0 = 8.253$ Å, $b_0 = 4.783$ Å and $c_0 = 8.540$ Å [5,6] and have a thickness of 500 Å. Two preferred orientations of [102] and [101] TiSi₂

can be epitaxially grown on (111) Si at local areas. The average grain sizes are 1.5, 4 and 4 μm for the samples annealed at intervals as described above and are denoted by A, B and C, respectively.

The bright-field TEM micrographs of the samples are shown in fig. 1. The growth rate of the grain size of samples B and C follows the diffusion-limit equation. The halt in the grain growth is believed to be due to the impurity drag effect [7], and/or the thickness inhibition effect [7]. It is interesting to note that the surface morphology degrades slightly with the increase of annealing time resulting from the outward precipitation of impurities [8,9].

To perform the resistivity and Hall constant measurement, the electrical lead wires were indium soldered with four contact pads in the form of a van der Pauw pattern [10]. A compact liquid-nitrogen cryostat (Oxford DN710) and a precise temperature controller with a precision of 0.05% (Oxford DTC2) were implemented for the temperature dependent

measurement. The current-voltage characteristic of the front and back surface of the sample indicates that the interface of the TiSi_2 film and the silicon substrate forms an ideal Schottky barrier which effectively blocks the current flow from TiSi_2 to the silicon substrate during van der Pauw measurement.

The temperature dependences of the electrical resistivity of TiSi_2 at an annealing temperature of 800°C for 6, 30 and 240 min are shown in fig. 2. The smooth appearance of curves B and C indicates that the resistivity of silicides follows Mathiessen's rule [11] as a normal metal, which is

$$\rho(T) = \rho_0 + \rho_1(T), \quad (1)$$

where ρ_0 is the residual resistivity due to collisions of carriers with mechanical imperfections and impurities, and $\rho_1(T)$ is the resistivity caused by thermal phonons. With the implication of phonon mode structure, the $\rho_1(T)$ can be expressed by the Bloch-Grüneisen law [12]. $\rho_1(T)$ approaches the ideal re-

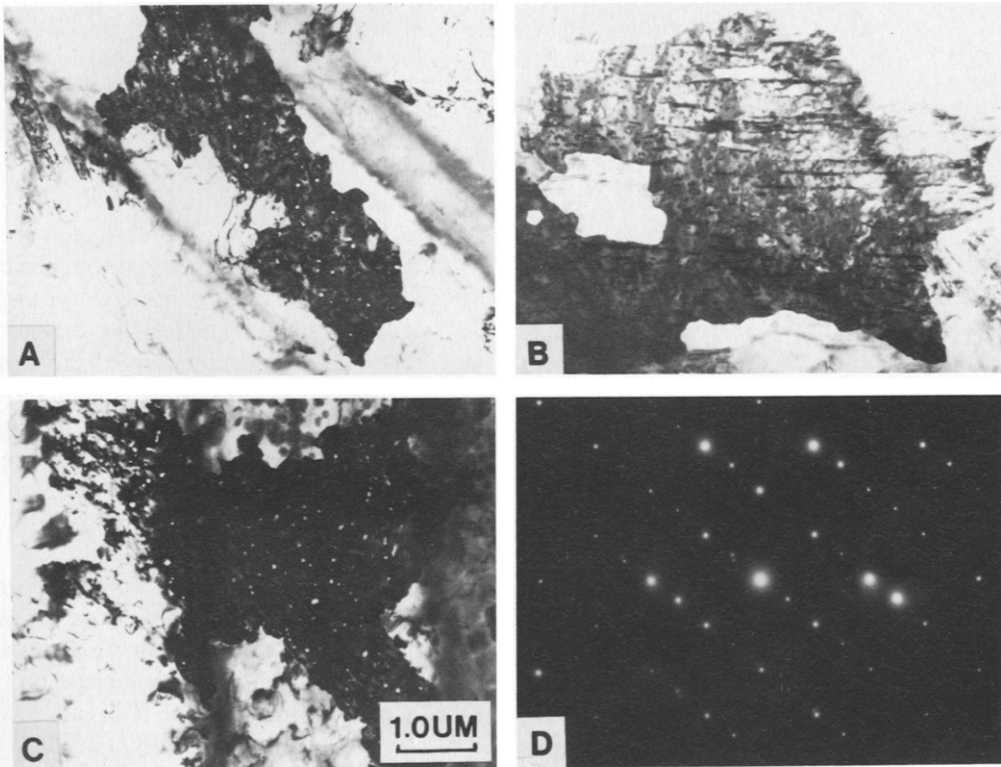


Fig. 1. Bright field micrographs of the $\text{C}_{54}\text{-TiSi}_2$ samples isothermally annealed at 800°C for (A) 6 min, (B) 30 min, and (C) 240 min, respectively. The same electron diffraction patterns are seen on all samples and are shown in (D).

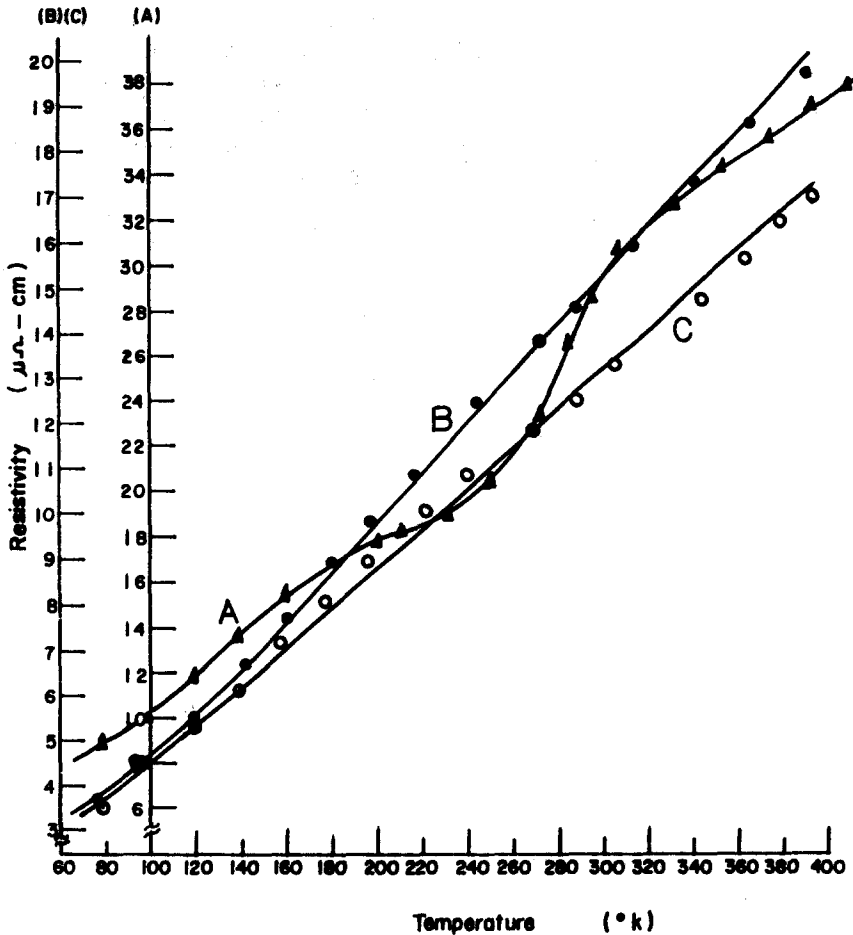


Fig. 2. Resistivities of TiSi_2 at various temperatures for a sample isothermally annealed at 800°C for (A) 6 min, (B) 30 min, and (C) 240 min, respectively. $\rho_0 = 3.26 \mu\Omega \text{ cm}$, $\theta = 450 \text{ K}$ for (B) and $\rho_0 = 3.10 \mu\Omega \text{ cm}$, $\theta = 510 \text{ K}$ for (C). The solid lines for (B) and (C) are fitted by the Bloch-Grüneisen law.

sistance limit, i.e. $\rho_1(T) \propto T/\theta^2$ as $T \gg \theta$, where θ is the Debye temperature. Allowing the parameters ρ_0 , and θ to vary, the least-mean square fit implies $\theta \approx 450\text{--}510 \text{ K}$, and $\rho_0 \approx 3\text{--}3.5 \mu\Omega \text{ cm}$ which are values compatible to the reported ones [4]. As pointed out before, the impurities contained in the silicide will segregate during epitaxial growth and precipitate on the surface. Although samples B and C have almost the same grain size their purities and surface morphologies are different implying different mean free paths and Debye temperatures. The slight deviation of slopes of the Bloch-Grüneisen plots for samples B and C clearly reveals their various intrinsic properties.

Curve A in fig. 2 indicates a striking dip of resistivity at a certain temperature. This anomalous behavior can be explained by the fact that insufficient annealing time might introduce localized magnetic moments due to unprecipitated atoms and ionized Ti atoms. Kondo [13] showed that the scattering by the exchange magnetic coupling has a negative temperature dependence on the resistivity, as

$$\rho_{\text{spin}} = c\rho_0 - c'J \ln T, \quad (2)$$

where J is the exchange energy. This spin resistivity combined with the positive phonon resistivity can give a dip. Schrieffer has demonstrated that the Kondo temperature can exist even up to the melting

points of metals [14]. The other mechanisms causing a negative temperature coefficient of the resistivity, phonon drag [15] and the Mooij correlation [16] which are important in semiconductors and heavily radiation damaged samples, respectively, are improper to silicides.

The temperature dependent Hall constant R_H of $TiSi_2$ is plotted in fig. 3 with the same annealing conditions as those of fig. 2. All the samples have the same character except that the absolute value of R_H decreases as the annealing time increases invoking a tendency of alternating the anisotropy of the carrier

life time. R_H increases gradually from the high temperature regions toward a maximum near 300 K, and then decreases sharply until it reverses sign where-upon the R_H curve becomes positive and flat.

Since the band structure and Fermi surface of silicides are still unknown, and even supposing that we knew the shape of the Fermi surface, the electron velocity for each value of k , the matrix elements for all scattering processes, and the phonon spectrum, a qualitative analysis of the resistivity and R_H is still very difficult. Here we try to apply Ziman's approximation [17] to interpret the increase of R_H as the

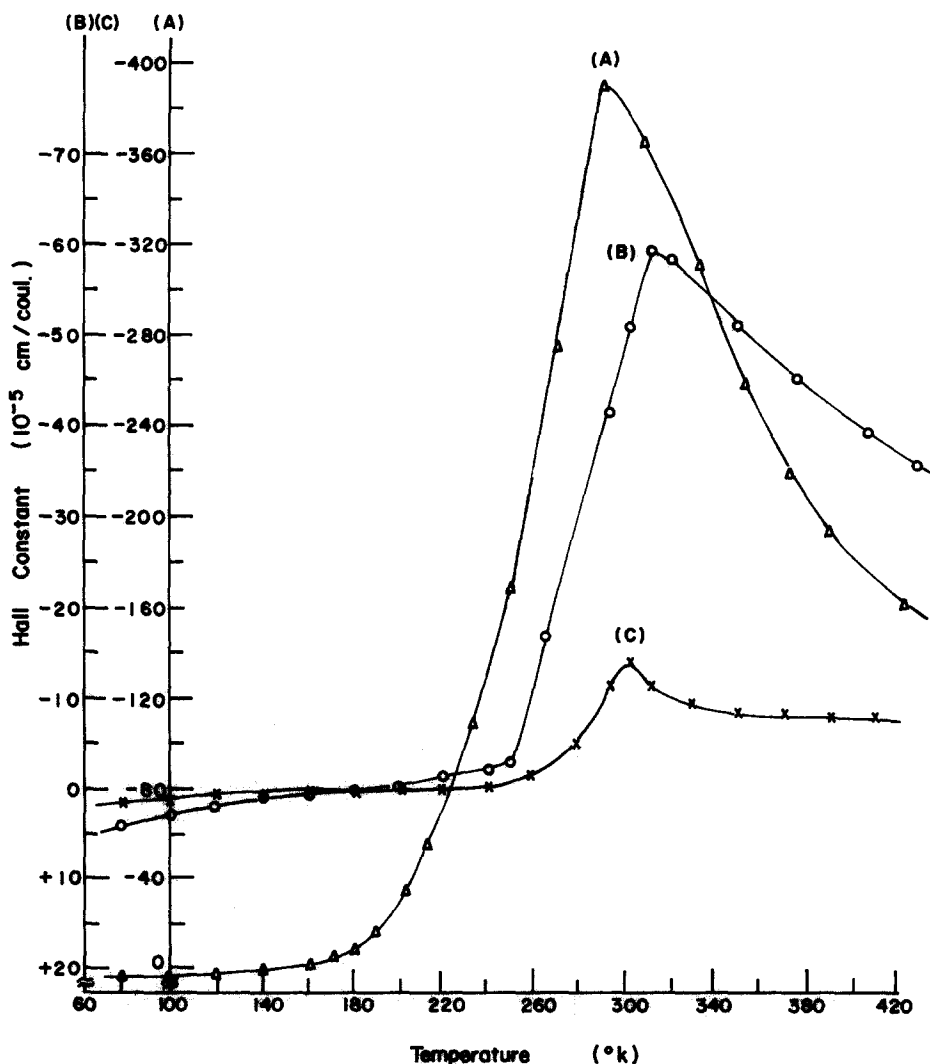


Fig. 3. Hall constants versus temperatures for the same samples as described above. The magnetic field is kept at 7000 G.

temperature decreased from the Debye temperature.

For polyvalent metals, the Fermi surface is multi-connected with the hole and electron orbits. The Hall constant at the low field limit for a cubic metal with anisotropic relaxation time $\tau(k)$ can be expressed by [18]

$$R_H = - \frac{12\pi^3}{cq} \times \frac{\int_B \tau_B^2(k) \nu_B^2(\overline{1/r}) ds + \int_N \tau_N^2(k) \nu_N^2(\overline{1/r}) ds}{[\int \tau_B(k) \nu_B ds + \int \tau_N(k) \nu_N ds]^2}, \quad (3)$$

where $\overline{1/r}$ is the mean value of the curvature of the Fermi surface at the point k , q is the electron charge, τ_B and τ_N are the average relaxation time on the belly and neck region of the Fermi surface, respectively, $\nu = n^{-1} \nabla_k \epsilon$ is the momentum derivation of the Fermi surface and ds is the surface element in momentum space. The anisotropic change of τ can be due to both normal and umklapp processes. The electrons on the neck region are dominantly scattered by the umklapp process since they are close to the Brillouin zone and can effectively be scattered between different zones.

The temperature dependence of τ_N on umklapp processes is not pronounced. On the other hand, the umklapp process on the belly region is strongly affected by the temperature. At high temperatures, the umklapp process is dominating both in τ_B and τ_N , therefore $\tau_B \approx \tau_N$, and their deviation becomes larger as the temperature decreases. Ziman in his early calculations for copper found that $\tau_B/\tau_N \approx 0.9$ for $T/\theta = 1$ and $\tau_B/\tau_N \approx 2.2$ for $T/\theta = 0.2$. It can be readily expected that the ratio of $(\tau_B^2 + \tau_N^2)/(\tau_B + \tau_N)^2$ increases as the deviation of τ_B and τ_N increases. Therefore, it is clear that R_H becomes greater as the temperature is reduced. However, τ_B cannot grow without limit. As the temperature decreased below 300 K, the excess growth of τ_B is frozen out, and the excess growth of τ_N is lengthened a little by the decreasing probability of umklapp processes, therefore R_H decreases again. At sufficient low temperatures, the τ_B/τ_N curve becomes flat because both of them are mostly contributed by the normal process.

In eq. (3), the sign of $\overline{1/r}$ depends on whether the normal to the Fermi surface is inward or outward corresponding to the contributions from the unfilled (hole) or filled (electron) states. The sign reversal of R_H as the temperature is reduced further can be

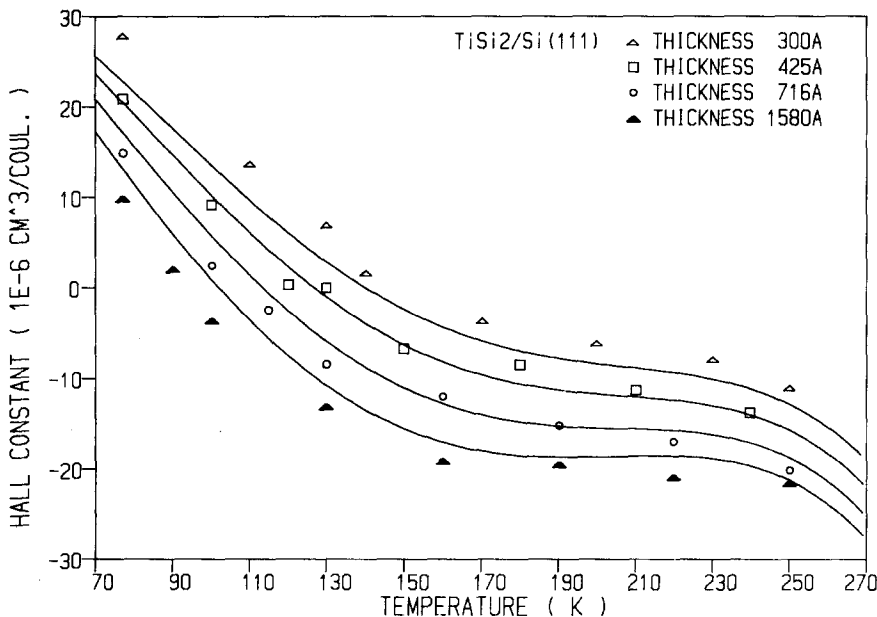


Fig. 4. Hall constants versus temperatures for samples annealed at 800°C for 240 min at various TiSi₂ thicknesses. The solid lines are the theoretical two-band calculations.

explained by the size effect. The two-band Hall constant for a compensated, low field limit (i.e. $\mu H \ll 1$) can be simplified to give (see ref. [18], p. 90)

$$R_H = \frac{r_H (\mu_h^2 N_h - \mu_e^2 N_e)}{|q| (\mu_h N_h + \mu_e N_e)^2}, \quad (4)$$

where r_H is the Hall factor, N_e and N_h are the electron and hole concentration, respectively, and μ_e and μ_h are their corresponding mobilities. As the temperature decreases, the mean free path of the carriers increases, and the anomalous skin effect becomes important. The carriers with higher mobility at high temperatures are predominantly affected by the size effect or their mobility is reduced more at low temperatures. Consequently the sign of R_H will be reversed at certain temperature. To examine the size effect, we have measured the thickness dependence on the Hall constants as shown in fig. 4. The sign reversal temperature increases as the silicide thickness decreases. The experimental data fit the theoretical calculation by the two-band model very well.

The size effect that controls the resistivity and Hall constant can be clearly seen as follows. For optical incident light, only electrons travelling nearly parallel to the surface can effectively absorb and screen the incident light, and the skin depth can be expressed by [19]

$$\rho \approx (\rho/\rho_{\text{eff}})l \approx (2\rho_{\text{eff}}/\omega\mu)^{1/2}, \quad (5)$$

where μ is the vacuum permeability, ω is the optical frequency and ρ_{eff} is the effective resistivity. The Hagen-Rubens formula [20] implies a relationship between ρ_{eff} and the optical reflectivity R by

$$R \approx 1 - (8\omega\epsilon_0\rho_{\text{eff}})^{1/2}, \quad (6)$$

where ϵ_0 is the permittivity in vacuum. The optical reflectance of TiSi_2 at $\lambda = 2.5 \mu\text{m}$ is about 89%, which corresponds to a skin depth of about 220 Å. The effective resistivity $\rho_{\text{eff}} > \rho$ implies agreement with the anomalous skin effect. The estimated mean free path is around 400 Å at $T = 300 \text{ K}$ which is comparable to the film thickness, and the size effect begins to intervene.

In conclusion, the departure of the Hall constant from nearly temperature independent below the Fermi temperature indicates that TiSi_2 deviates from free electron model. The size effect may possibly solve the sign reversal of R_H . A rough estimation of carrier density n and relaxation time τ from $n \approx 1/R_H e$ at the flat value of R_H , and $\tau = m^*/ne^2\rho$ would give $n \approx 8.33 \times 10^{22} \text{ cm}^{-3}$, and $\tau = 3.6 \times 10^{-15} \text{ s}$ which are values close to those of normal metals.

This work was supported by the National Science Council of the Republic of China.

References

- [1] R.T. Tung, A.F.J. Levi and J.M. Gibson, *J. Vac. Technol. B* 4 (1986) 1435.
- [2] M.S. Fung, H.C. Cheng and L.J. Chen, *Appl. Phys. Lett.* 47 (1985) 1312.
- [3] M.E. Alperin and T.C. Hollaway, *IEEE J. Solid-State Circuits* SC-20 (1985) 61.
- [4] V. Malhotra, T.L. Martin and J.E. Mahan, *J. Vac. Sci. Technol. B* 2 (1984) 10.
- [5] Kung Lee and J.T. Lue, *Phys. Lett. A* 125 (1987) 271.
- [6] I.C. Wu and L.J. Chen, *J. Appl. Phys.* 60 (1986) 3172.
- [7] R.W. Cahn, *Physical metallurgy* (Elsevier, Amsterdam, 1983) pp. 1654-1656.
- [8] M. Berti, A.V. Drigo, C. Cohen, J. Sisjka, G.G. Bentin, R. Nipoti and S. Guerri, *J. Appl. Phys.* 55 (1984) 3558.
- [9] P. Merchant and J. Ameno, *J. Vac. Sci. Technol. B* 2 (1984) 762.
- [10] P.M. H. Emenger, *Rev. Sci. Instrum.* 44 (1973) 698.
- [11] C. Kittel, *Introduction to solid state physics*, 5th Ed. (Wiley, New York, 1976) p. 171.
- [12] J.M. Ziman, *Electrons and phonons* (Oxford Univ. Press, Oxford, 1960).
- [13] J. Kondo, *Solid State Phys.* 23 (1969) 184.
- [14] J.R. Schrieffer, *J. Appl. Phys.* 38 (1967) 1143.
- [15] K. Seeger, *Semiconductor physics* (Springer, Berlin, 1985) p. 85.
- [16] J.H. Mooij, *Phys. Stat. Sol. (a)* 17 (1973) 521.
- [17] J.M. Ziman, *Phys. Rev.* 121 (1961) 1320.
- [18] C.M. Hurd, *The Hall effect in metals and alloys* (Plenum, New York, 1972).
- [19] F. Wooten, *Optical properties of solids* (Academic Press, New York, 1972) p. 94.
- [20] G.R. Fowles, *Introduction to modern optics*, 2nd Ed. (Holt, Rinehart and Winston, New York, 1975) p. 168.